Chapter 5

Free-Space Transmission Method for the Characterization of Dielectric and Magnetic Materials at Microwave Frequencies

Irena Zivkovic and Axel Murk

Additional information is available at the end of the chapter

http://dx.doi.org/10.5772/51596

1. Introduction

Materials that absorb microwave radiation are in use for different purposes: in anechoic chambers, for electromagnetic shielding, in antenna design, for calibration targets of radiometers, etc. It is very important to characterize them in terms of frequency dependent complex permittivity and permeability for a broad frequency range.

Widely used absorbing materials are CR Eccosorb absorbers from Emerson&Cuming Company. Permittivity and permeability of these materials are characterized by manufacturer up to frequency of 18GHz, but it is important (in absorbing layer design purposes, for example) to know these values at much higher frequencies.

In this work we will present new method, retrieved results and validation for complex and frequency dependent permittivity and permeability parameter extraction of two composite, homogeneous and isotropic magnetically loaded microwave absorbers (CR Eccosorb). Permittivity and permeability are extracted from free space transmission measurements for frequencies up to 140GHz. For the results validation, reflection measurements (samples with and without metal backing) are performed and are compared with simulations that use extracted models. The same method is applied in complex and frequency dependent permittivity model extraction of commercially available epoxies Stycast W19 and Stycast 2850 FT.

The proposed new method solves some shortcomings of the popular methods: extracts both permittivity and permeability only from transmission parameter measurements, gives good results even with noisy data, does not need initial guesses of unknown model parameters.

2. Definition of permittivity and permeability

In the absence of dielectric or magnetic material, there are the following relations:

$$D = \varepsilon_0 \cdot E \tag{1}$$

$$B = \mu_0 \cdot H \tag{2}$$

where D is electric induction, E is electric field, B is magnetic induction and H is magnetic field. ε_0 and μ_0 are permittivity and permeability of free space, respectively. Values of ε_0 and μ_0 are: ε_0=8.854 $\cdot$ 10^{-12} [$\frac{F}{m}$] and μ_0=4 $\cdot$ π $\cdot$ 10^{-7} [$\frac{V \cdot s}{A \cdot m}$]. Dielectric permittivity and magnetic permeability of the free space are related to each other in the following way:

$$c^2 = \frac{1}{\mu_0 \cdot \varepsilon_0} \tag{3}$$

where c is the speed of light in a vacuum and its value is $c \approx 3 \cdot 10^8$ [$\frac{m}{s}$].

If an electromagnetic field interacts with material that is dielectric or magnetic, equations (1) and (2) can be represented as follows:

$$D = \varepsilon_0 \cdot \varepsilon \cdot E \tag{4}$$

$$B = \mu_0 \cdot \mu \cdot H \tag{5}$$

where ε and μ are relative permittivity and permeability of the observed material and can be real or complex numbers (Eq. (6) and (7)).

$$\varepsilon = \varepsilon^{'} - j \cdot \varepsilon^{''} \tag{6}$$

$$\mu = \mu^{'} - j \cdot \mu^{''} \tag{7}$$

where j is imaginary unit and j^2= -1.

Permittivity is a quantity that is connected to the material's ability to transmit ('permit') an electric field. The real part, $\varepsilon^{'}$, is related to the ability of material to store energy, while the imaginary part, $\varepsilon^{''}$, describes losses in material. Permeability is a parameter that shows the degree of magnetization that a material obtains in response to an applied magnetic field. Analogous to the real and imaginary permittivity, the real permeability, $\mu^{'}$, represents the energy storage and the imaginary part, $\mu^{''}$, represents the energy loss term.

The polarization response of the matter to an electromagnetic excitation cannot precede the cause, so Kramers-Kronig relations given by Eqs. (8) and (9) ([8]), for the real and imaginary parts of permittivity (permeability) have to be fulfilled.

$$\varepsilon^{'}(\omega) = \varepsilon_\infty + \frac{2P}{\pi} \int_0^\infty \frac{\omega^{'} \epsilon^{''}(\omega^{'})}{\omega^{'2} - \omega^2} d\omega^{'} \tag{8}$$

$$\varepsilon^{''}(\omega) = -\frac{2\omega P}{\pi} \int_0^\infty \frac{\epsilon^{'}(\omega^{'}) - \varepsilon_\infty}{\omega^{'2} - \omega^2} d\omega^{'} \tag{9}$$

where ω is angular frequency, ε_∞ is permittivity when $\omega \to \infty$ and P stands for the Cauchy principal value. The convention of the time variation is $\exp(j\omega t)$ and the time derivative is equal to multiplication by $j\omega$.

The Kramers-Kronig relations connect the real and imaginary parts of response functions. If we know the real/imaginary part of permittivity/permeability on the complete frequency range, the other unknown part can be calculated using the Kramers-Kronig relations. Because

of the causality constraint, when we develop models for frequency dependent permittivity or permeability, they must satisfy the Kramers-Kronig relations.

3. Modeling of frequency dependent permittivity and permeability

Dielectric and magnetic loss mechanisms can be represented in the frequency domain as relaxation or resonant type. In the microwave frequency range dielectric losses usually exhibit relaxation behavior ([1]), while magnetic losses exhibit resonant behavior ([6]), ([7]).

3.1. Debye relaxation model

The simplest one pole Debye relaxation model is represented with the Eq. (10).

$$\varepsilon(f) = \varepsilon_\infty + \frac{\varepsilon_s - \varepsilon_\infty}{1 + j\frac{f}{f_r}} \tag{10}$$

where ε_s is a static dielectric permittivity, ε_∞ is permittivity at infinite frequency (optical permittivity), f_r is relaxation frequency. Figure 1 gives an example of Eq. (10) with ε_∞ = 7, ε_s = 17 and f_r = 9 (in GHz). Imaginary part of permittivity in Figure 1 is represented as a positive number.

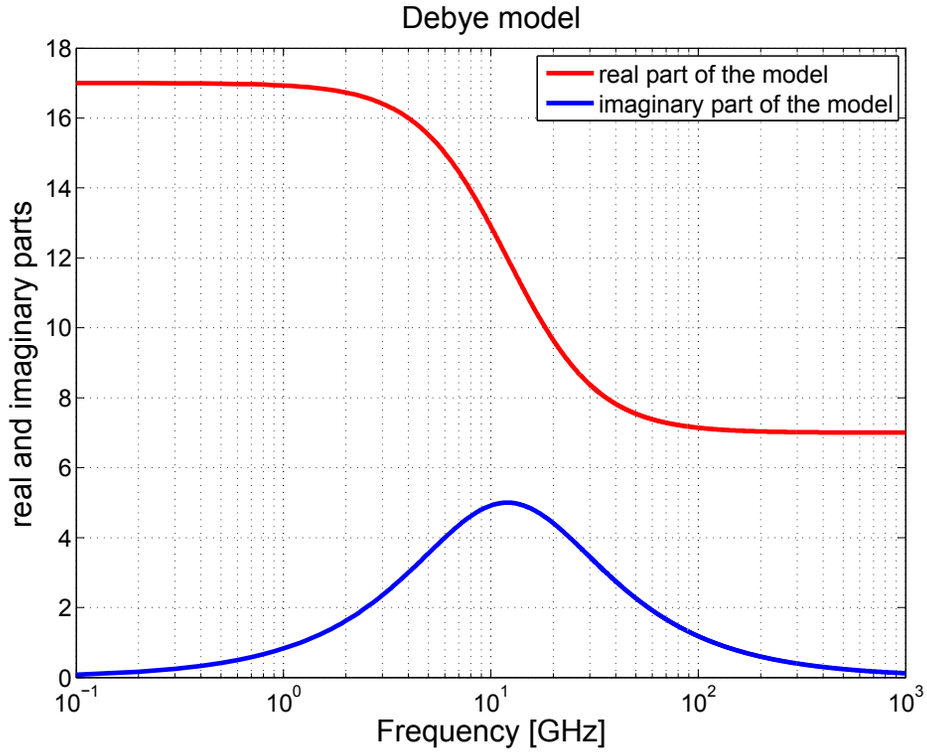

Figure 1. Real and imaginary permittivity represented with Debye model.

There are some modified Debye relaxation models that include asymmetrical and damping factors ([2]). These models are Cole-Cole, Cole-Davidson and Havriliak-Negami. They are

presented with equations (11), (12) and (13), respectively.

$$\varepsilon(f) = \varepsilon_\infty + \frac{\varepsilon_s - \varepsilon_\infty}{1 + j\left(\frac{f}{f_r}\right)^{1-\alpha}} \tag{11}$$

$$\varepsilon(f) = \varepsilon_\infty + \frac{\varepsilon_s - \varepsilon_\infty}{\left(1 + j\left(\frac{f}{f_r}\right)\right)^{\beta}} \tag{12}$$

$$\varepsilon(f) = \varepsilon_\infty + \frac{\varepsilon_s - \varepsilon_\infty}{\left(1 + j\left(\frac{f}{f_r}\right)^{1-\alpha}\right)^{\beta}} \tag{13}$$

The terms α and β are empirical parameters and their values are between 0 and 1. α is a damping factor and describes the degree of flatness of the relaxation region. β is an asymmetric factor and describes relaxation properties asymmetric around relaxation frequency.

In our work, we will model dielectric permittivities of the samples with Debye relaxation model given with Eq. (10).

3.2. Lorenzian resonance model

Lorenzian resonant model is represented with Eq. (14) and Eq. (15). Graphical representation of Eq. (14) is in Figure 2 which is an example with μ_s = 9 and f_r = 25 GHz. Imaginary part of permeabilty in Figure 2 is represented as positive number.

$$\mu(f) = 1 + \frac{\mu_s - 1}{\left(1 + j\frac{f}{f_r}\right)^2} \tag{14}$$

where μ_s is static permeability and f_r is resonant frequency.

$$\mu(f) = 1 + \frac{\mu_s - 1}{1 + j\frac{f}{f_{r1}} - \left(\frac{f}{f_{r2}}\right)^2} \tag{15}$$

Eq. (15) comes when we develop Eq. (14). If $2f_{r1} = f_{r2}$, Eq. (14) is equivalent to the Eq. (15).

Damping and asymmetric factors are introduced in the following equations ([2]).

$$\mu(f) = 1 + \frac{\mu_s - 1}{1 + j\gamma\frac{f}{f_r} - \left(\frac{f}{f_r}\right)^2} \tag{16}$$

$$\mu(f) = 1 + \frac{\mu_s - 1}{\left(1 + j\gamma\frac{f}{f_r} - \left(\frac{f}{f_r}\right)^2\right)^k} \tag{17}$$

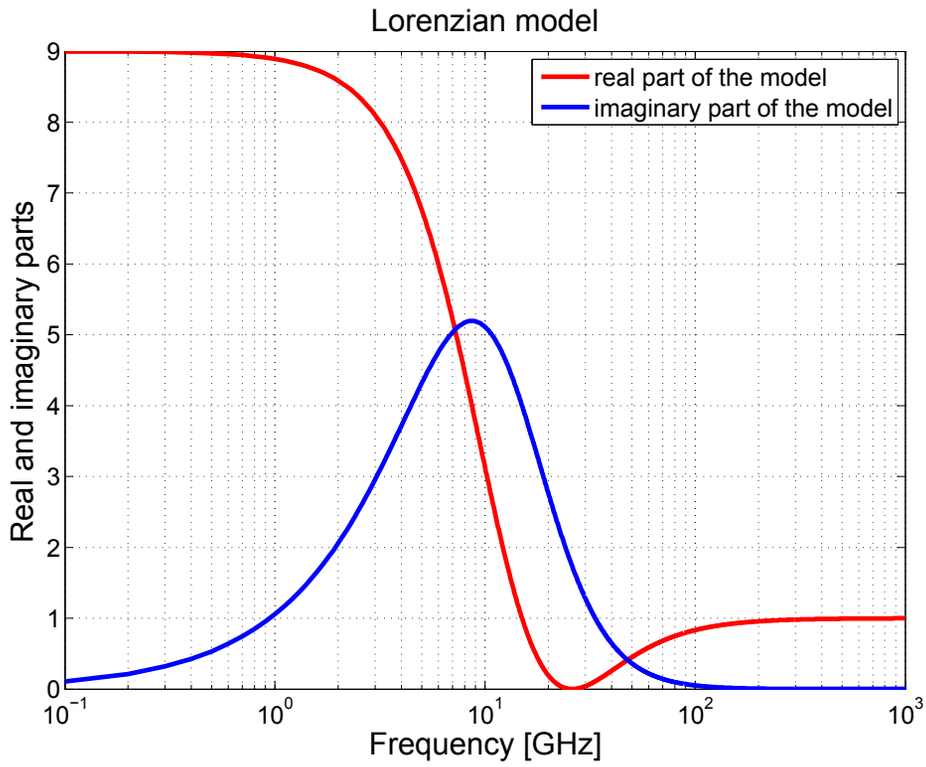

Figure 2. Real and imaginary permeability represented with Lorenzian model.

The γ factor is an empirical constant and represents damping factor of a resonance type. The term k is also an emirical constant which values are between 0 and 1. It is asymmetrical factor of a resonance type.

In our work we will model complex permeability with Lorenzian resonant model and we will 'tune' models by involving empirical factors k and γ.

4. Scattering parameters measurements and methods for permittivity and permeability extractions

When an electromagnetic wave interacts with a material sample of finite thickness, reflected and transmitted signals can be registered. On the air-material sample interface, part of the signal reflects back, while the other part penetrates into the material. Inside the material the signal attenuates and on the second material sample-air interface part of the signal reflects back into the sample while the other part continues to go forward, ie. transmits. Scattering parameters (transmission and reflection) depend on permittivity (ε) and permeability (μ) of the material and by measuring them we can extract ε and μ.

4.1. Transmission/reflection waveguide measurements

Coaxial line, rectangular and cylindrical waveguide measurements are widely used broadband measurement techniques because of their simplicity ([5]), ([3]). In these methods, the material sample is placed into the section of a waveguide or a coaxial line and scattering parameters are measured with network analyzer.

A major problem in transmission line measurements is the possible existance of air gaps between the sample and walls of the waveguide. Samples must be very precisely machined. For example, in X band waveguide measurements (8 to 13GHz, waveguide dimensions 22.9 x 10.2mm), uncertainty in the sample cutting should be in the range of 20μm ([5]).

Important problems with transmission line measurements are also half wavelength resonance and overmoding ([5]). Propagation of single mode resonates at integer multiplication of one half wavelength in the sample. Some techniques for permittivity and permeability extractions break down in the presence of half wavelength resonance. An additional problem is overmoding which means appearance and propagation of higher order modes in the closed waveguide structure. In waveguides and coaxial lines the asymmetry of the sample and machining precision promotes higher order mode propagation. Their appearance determines dips in the reflection coefficient caused by resonances of the excited higher order mode which cause failure of, for example, point by point technique for permittivity and permeability extraction.

4.1.1. Free space measurements

Free space measurements give a noninvasive broadband technique for transmission and reflection parameters measurements. Scattering parameters are measured of the sample that is plane parallel. Measurement setup consists of two identical antennas that operate in certain frequency range and network analyzer. For measurements, corrugated horn antennas can be used. Antennas are aligned and one of them transmits signal while the other antenna works as receiver. Material sample is placed between the two antennas, the incident signal passes through material and is registered by the other antenna. On that way, free space transmission coefficient is measured. Depending on frequency and sample size, focusing lenses can be used.

For reflection measurements, one antenna is connected to the network analyzer via directional coupler. The antenna is sending signal and also measures reflection from the sample that is in front of the antenna.

4.2. Methods for permittivity and permeability extractions

4.2.1. Analytical approach - Nicholson Ross Weir derivation

The Nicholson Ross Weir (NRW) derivation is an analytical method that calculates permittivity and permeability from measured S_{11} and S_{21} parameters. Dependence of scattering parameters from material properties is derived considering multiple reflections of the wave incident upon the air-sample interfaces when the sample is in free space or inside of waveguide ([5]), ([3]). Equations (18) to (29) represent short version of the NRW derivation for scattering parameters measured in free space. If we consider a system of air/sample/air, then the incident wave travels and a first partial reflexion on the air-sample interface occurs. The remaining portion of the signal continues to travel through the sample and on the second air-sample interface part of the signal transmits and the other part reflects back and travel through the sample toward the first air-sample interface. After simplification of expressions that include all terms of multiple reflections and transmissions, the final expression for the

total reflection parameter, S_{11}, and the total transmission parameter, S_{21}, are given with Eq. (18) and Eq. (19).

$$S_{11} = \frac{G1 \cdot (1 - z^2)}{(1 - G1^2 \cdot z^2)} \tag{18}$$

$$S_{21} = \frac{z \cdot (1 - G1^2)}{(1 - G1^2 \cdot z^2)} \tag{19}$$

$$z^2 = e^{-2 \cdot j \cdot \gamma \cdot d} \tag{20}$$

$$G1 = \frac{(Z - 1)}{(Z + 1)} \tag{21}$$

$$Z = \sqrt{\frac{\mu}{\varepsilon}} \tag{22}$$

where z is unknown variable that depends on the propagation constant γ, d is the sample thickness, $G1$ is the first partial reflection on the air-sample interface, Z is characteristic impedance of the material and depends on ε and μ of the material as given with Eq. (22). Relation of the propagation constant γ with ε and μ of the material is given by Eq. (23).

$$\gamma = \frac{j \cdot 2 \cdot \pi \cdot \sqrt{\varepsilon \cdot \mu}}{\lambda} \tag{23}$$

$$\lambda = \frac{c}{f} \tag{24}$$

where λ is a free space wavelength, c is speed of light in vacuum and f is the frequency.

$$\gamma = -\frac{1}{d} \cdot log \frac{1}{z} \tag{25}$$

From the Eq. (20), γ is expressed as a function of z and d (Eq. (25)). d is material slab thickness and z is calculated from Eq. (18) and Eq. (19).

N_m is material's refractive index and can be expressed in terms of permittivity and permeability as:

$$N_m = \sqrt{\mu \cdot \varepsilon} \tag{26}$$

By combining Eq. (23) and Eq. (26) we obtain expression for material's refractive index (Eq. (27)). $G1$ is expressed as a funcion of S_{11} and S_{21} and Z is expressed as a function of $G1$. Finally, ε and μ are expressed as a functions of N_m and Z (Eqs. (28) and (29)).

$$N_m = \frac{-j \cdot \lambda \cdot \gamma}{2 \cdot \pi} \tag{27}$$

$$\varepsilon = \frac{N_m}{Z} \tag{28}$$

$$\mu = N_m \cdot Z \tag{29}$$

The numerical shortcoming of the NRW derivation comes from Eq. (25) where the natural logarithm of a complex number has to be calculated and there is no unique solution. The

choice of the correct root is essential in order to find the correct solution of the complex permittivity and permeability. Comparison of the calculated and measured time delays can help in resolving this problem ([5]). The second problem arises when S_{11} and S_{21} are noisy. The NRW derivation calculates ε and μ from S_{11} and S_{21} for each frequency point. Small measurement errors in the dataset result in significant errors on the calculated values of ε and μ. Figure 4 represents an example of permittivity and permeability calculation with NRW algorithm when S_{11} and S_{21} are noisy. Frequency dependent permittivity and permeability represented with Debye and Lorenzian models are included into the Fresnel's equations based algorithm. Fresnel's equations based algorithm then calculates S_{11} and S_{21} (Figure 3). Noise with relative amplitude of 0.05 is added to simulated S_{11} and S_{21}. Figure 4 represents original ε and μ as well as ε and μ calculated with NRW derivations.

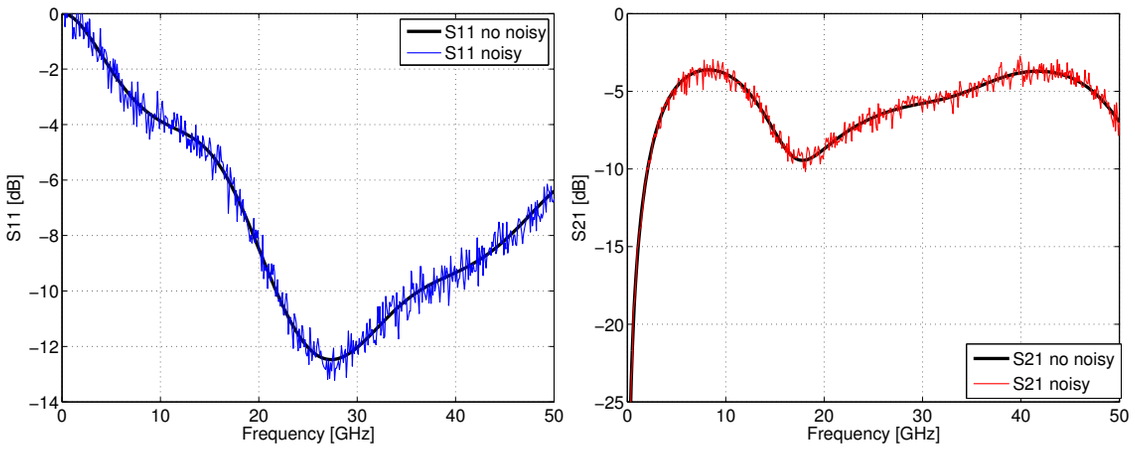

(a) (b)

Figure 3. Noisy S_{11} and S_{21} that are used for permittivity and permeability calculations with NRW derivation.

4.2.2. Numerical approach

Taking various linear combinations of scattering parameters it is possible to calculate unknown permittivity and permeability ([5]). In order to obtain values for both parameters, we need to have two different measurements of scattering parameters: S_{11} and S_{21} measured on one material sample, or one port shorted circuit line measurement of material sample at two different positions in the line, or measurement of one scattering parameter but for the same material and two different thicknesses, etc. For the root determination of the equations (that are similar to the NRW equations) Newton's numerical method can be used ([5]). This iterative approach works well if good initial guesses are available.

One of the numerical methods for both permittivity and permeability determination is based on nonlinear least square optimization technique and is described in details in ([4]). Complex permittivities and permeabilities are represented as a sum of resonance and relaxation terms. Measured scattering parameters are fitted with simulations in the nonlinear least square sense and unknown free parameters from permittivity and permeability models are extracted. It is important to have a good initial guesses of the unknown parameters contained in the ε and μ models in order of optimization to converge to the correct solution. The initial guesses should

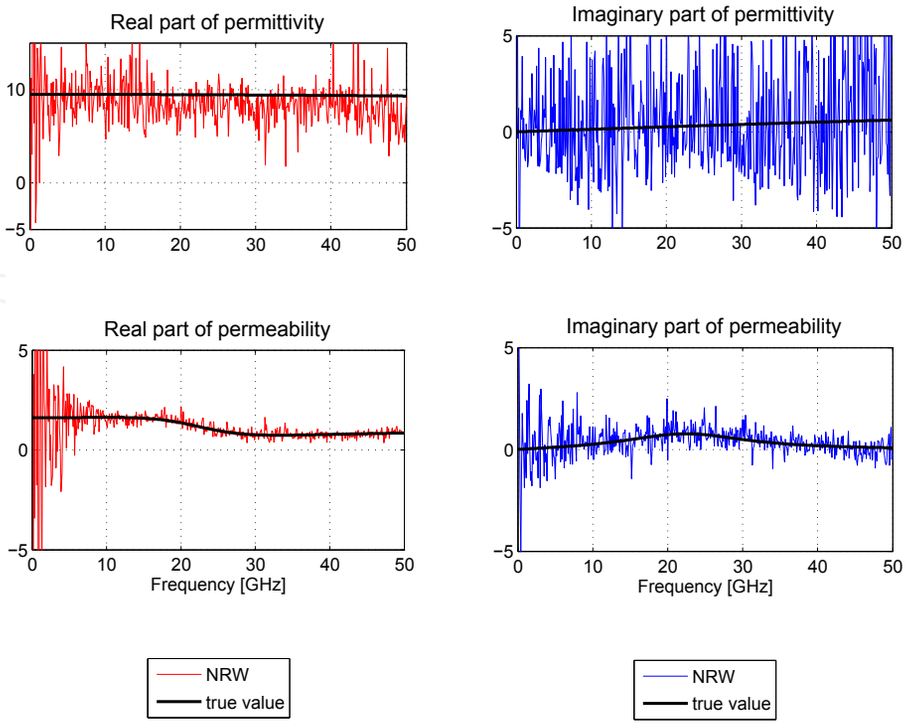

Figure 4. Real and imaginary permittivity and permeability calculated from noisy S_{11} and S_{21} by using NRW derivation. Black line represents original values of permittivity and permeability which were used to simulate the S-parameters.

be within 10 to 20% of the true values. The problem is when we examine material without any *a priori* knowledge about its properties, then we are not able to give good initial guesses of its unknown parameters.

5. Developed method for permittivity and permeability extraction

There are uncertainties in free space scattering parameters measurements and they have some frequency dependence with higher frequencies having larger uncertainties. More sensitive to measurement uncertainties is the S_{11} parameter ([5]), ([3]), ([4]). For that reason we use free space transmission S_{21} parameter for permittivity and permeability model retrival, and free space reflection (S_{11} and S_{11m}, reflections from the samples with and without metal backing) parameter for extracted permittivity and permeability models validation.

Measurements and parameters extraction are concerned Eccosorb CR110, CR114 and CRS117 samples. The CR materials are a two composite-mixture of epoxy and magnetic inclusions and are not flexible materials. A higher product number indicates a higher filling factor of the magnetic loading and therefore the higher absorption. The CRS materials are flexible silicon based materials. They should have the same electrical properties as hard epoxy based materials.

In our work we use the assumption that all material samples are two composite, homogeneous and isotropic. Dimensions and densities of the samples that we examined are summarized in the Table 1. The samples are 2.00mm thick with plane parallel circular surfaces.

$Eccosorb\ material$	$Diameter\ [mm]$	$Density\ [\frac{g}{cm^3}]$
$CR110$	91.70	1.60
$CR114$	92.80	2.88
$CRS117$	75.60	4.16

Table 1. CR samples dimensions and densities

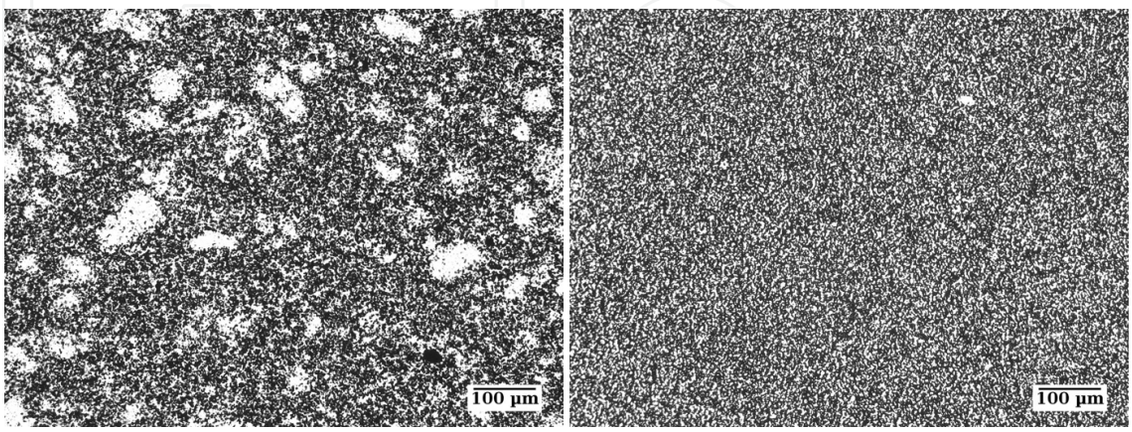

(a) (b)

Figure 5. Microscope view of CR110 (left) and CR114 (right) samples. Photographs are taken with the same magnification for both samples.

Figure 5 represents microscopic view of CR110 and CR114 materials. Different densities of materials can be noticed. For these images, both samples had been polished to approximately 20μm thick slabs.

5.1. Scattering parameters measurements

5.1.1. Transmission measurements

Free space transmission measurements are performed with a setup explained in section 4.1.1. Measurements are performed at frequencies from 22 to 140GHz. Low frequency measurements are limited by the sample size.

Instead of placing material sample between two aligned antennas, we do transmission measurements by placing sample on the aperture of one of the antennas. Corrugated horn antennas are used because they have less near field effects at the aperture than rectangular horns. Calibration for S_{21} measurements is done with 'through' measurement Eq. (30). 'Through' signal is measured when antennas are separated only by air, without sample.

$$S_{21cal} = \frac{S_{21meas}}{S_{21through}} \tag{30}$$

where S_{21cal} is the calibrated signal, S_{21meas} is the transmission parameter measured through material sample and $S_{21through}$ is the through measurement, with the signal received by the other antenna when no sample is between the two antennas.

5.1.2. Reflection measurements

Reflection measurements are performed by placing the material sample on the aperture of the antenna. We did two types of reflection measurements: with sample and metal backing (a metalic reflector placed behind the sample) placed on the aperture and only with the sample placed on the antenna's aperture.

The antenna is connected to the vector network analyzer through directional coupler. For calibration purposes we measure the reference signal (metal plate is on the aperture of the antenna, 100% reflection) and the signal when low reflectivity pyramidal foam absorber ($S_{11foam} <$ -50dB) is in front of the antenna's aperture (to calibrate directivity). Calibration of the measured reflection parameter is given by Eq. (31).

$$S_{11cal} = \frac{S_{11meas} - S_{11foam}}{S_{11alu} - S_{11foam}} \tag{31}$$

where S_{11cal} is the calibrated signal, S_{11meas} is the measured reflection parameter of the sample, S_{11foam} is the measured reflection when foam absorber is on the top of aperture and S_{11alu} is reference reflection measurement, when metal is on the aperture of the antenna.

5.2. Procedure for parameters extraction

We do not have any information about epoxy and magnetic inclusions properties. Our assumptions on the examined material samples are described as follows:

- the samples are two component composite materials (this is given by manufacturer, samples are mixtures of dielectric matrix and magnetic particles);
- inclusions are smaller when compared to the wavelength;
- the material is isotropic and homogeneous at macroscopic scale.

Epoxy is low loss dielectric material, while magnetic inclusions have magnetic and also dielectric properties. With previous assumptions and according to ([8]), if magnetic dispersion of inclusions is of resonance Lorenzian type than dispersion law for the composite will be Lorenzian as well. Analogous to that, dielectric dispersion of the composite can be modeled with relaxation Debye model.

At high frequencies ($>$ 60-70GHz) there are no magnetic losses because magnetization is not possible since applied field is very fast and magnetic domains cannot follow the field. Permeability is equal to 1. It means that material samples exhibit only dielectric losses. We model dielectric losses with simple Debye model (Eq. (11)). Next step is to fit measured transmission parameter, with simulated S_{21}, both amplitude and phase. Fitting is based on minimization of the differences (in both amplitude and phase) between simulated and measured transmission data. Model of free space propagation is required to relate the material properties (permittivity and permeability) to the transmission (reflection) parameters. For that purpose we use routine based on Fresnel's equations. There are three unknowns in Debye model for permittivity calculation, ε_s, ε_∞ and f_r. Static permittivity, ε_s, is calculated for all samples by measuring capacitance of the sample at very low frequency. We

measure the sample's capacitance in a calibrated capacity bridge operating between 10Hz and 20kHz. Capacitance measurement works good if wavelength is much longer then the sample thickness. It is satisfied in our case because capacitance measurements are performed at 1kHz frequency and samples thicknesses are 2mm. One problem in capacitance measurements is given by the fringing fields. To eliminate them, we measure capacitance of the sample C and then capacitance of the capacitor with air instead of material sample C_{air}. Static permittivity ε_s is expressed by Eq. (32).

$$\varepsilon_s = \frac{C}{C_{air}} \tag{32}$$

where C is the measured capacitance of the material sample and C_{air} is the capacitance between parallel capacitor plates which are separated for a distance equal to the thickness of the material sample, but instead of material there is air.

We include measured ε_s into permittivity Debye model. The next step is to do measured and simulated data fitting at high frequencies (μ=1), both amplitude and phase, and to extract two other unknown parameters of Debye model, f_r and ε_∞. Once we have full Debye dielectric permittivity model, we can extract permeability.

Starting guess is that permeability of the CR110 sample satisfies Debye relaxation model. As a matter of fact, CR110 is the sample with the smallest amount of magnetic inclusions so permeability behavior should change from resonance to relaxation. Permeability models of CR114 and CRS117 samples are presumed to be of Lorenzian type. With these guesses, we do fitting of measurements and simulations at frequencies where permeability is different than 1, while for permittivity we use a model extracted in the previous step (from fitting with high frequency data). From fitting, we obtain free parameters of presumed permeability models.

Figure 6 represents measured and fitted amplitude and phase of examined Eccosorb samples. A phase offset of one π (Figure 6 (b)) has been applied between phases of different samples for clarity.

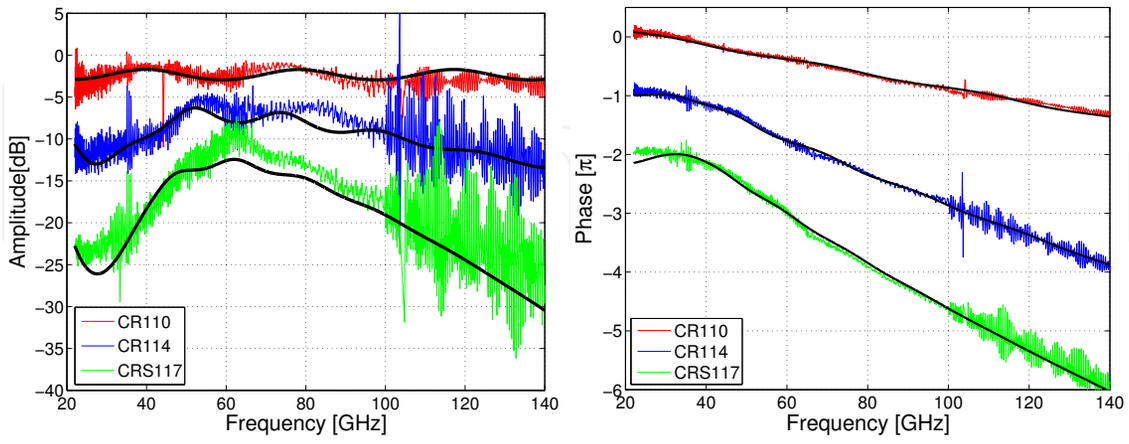

(a) (b)

Figure 6. Measured and fitted transmission parameter amplitudes (a) and phases (b) of CR110, CR114 and CRS117 samples.

5.3. Extracted permittivity and permeability of CR Eccosorb absorbers and results validation

To validate extracted models for both permittivity and permeability, we compare simulated reflection parameters (samples with and without metal backing) with measurements. Comparisons are presented in Figures 7 and 8 and good agreement between measurements and simulations is achieved. Reflection measurements are performed in Ka, U and W band.

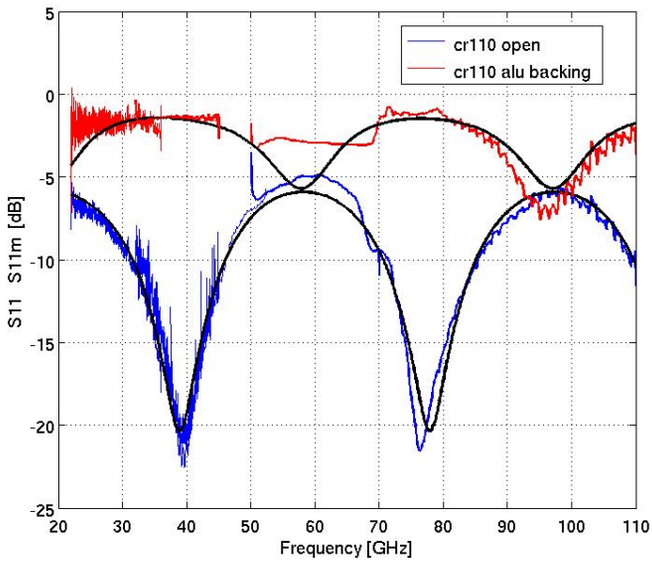

Figure 7. Measured and simulated reflection coefficient of CR110 absorber, with and without metal backing. Simulated reflections are represented with black solid line.

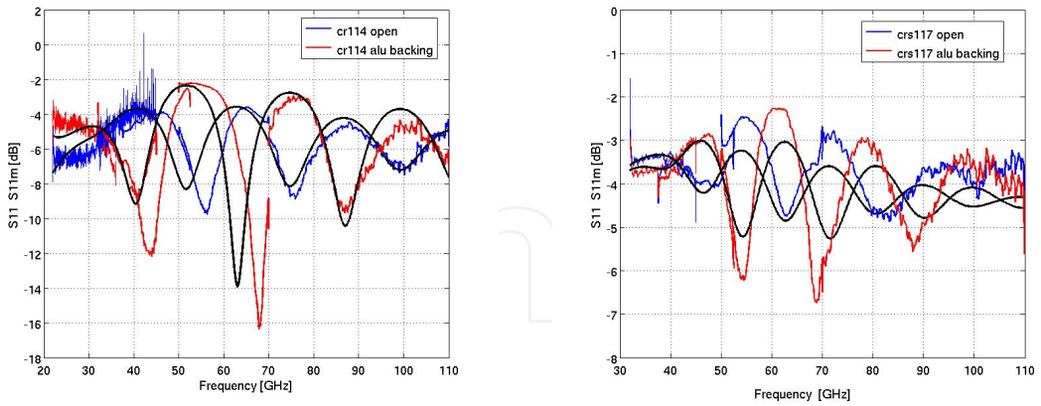

(a) (b)

Figure 8. Measured and simulated reflection coefficient of CR114 (a) and CRS117 (b) absorbers, with and without metal backing. Simulated reflections are represented with black solid line.

There are some inconsistencies in measurements in different frequency bands. That could come from the fact that we used different corrugated horn antennas for different frequency bands. Another possible source for the inconsistency in measurements can be caused by the

presence of the air gaps between samples and metal backing. Small air gaps exist because some of the examined samples are not completely flat, but are slightly bended.

By looking in amplitude behavior of transmission measurements (Figure 6 (a)) we can say that if permittivities and permeabilities are not frequency dependent, transmission coefficient decreases with increasing frequency. The fact that measured transmission coefficient decreases in some frequency range and increases in the other, says about frequency dependent material parameters.

Figures 9 and 10 represent extracted frequency dependent real and imaginary parts of permittivity and permeability of examined samples. As we mentioned, CR110 sample is low loss material with very small amount of magnetic particles that can produce losses. Because of the small concentration of magnetic particles, magnetic loss mechanism is transformed from resonance to relaxation (which is seen in Figure 10 (b), imaginary part of permeability). Both CR114 and CRS117 materials show Debye relaxation model for permittivity and Lorenzian model for permeability. The difference is that CRS117 material contains more magnetic inclusions compared to CR114 and thus showing the highest value of imaginary part of permeability.

One very important fact is that permeability of magnetic materials (in the range from 0 up to GHz frequencies) can contain one or multiple dispersion areas ([9]), ([10]). Below 20GHz we did not perform scattering measurements, so we have no data to be used in the fitting procedure. Furthemore, we do not have any information about materials that we examine so we cannot be completely sure of the correctness of the reconstructed model for permeability behavior at frequencies below 20GHz. For that reason, retrieved permittivity and permeability data should be used in the frequency range from 20 to 140GHz, ie. that adopted in the fitting procedure.

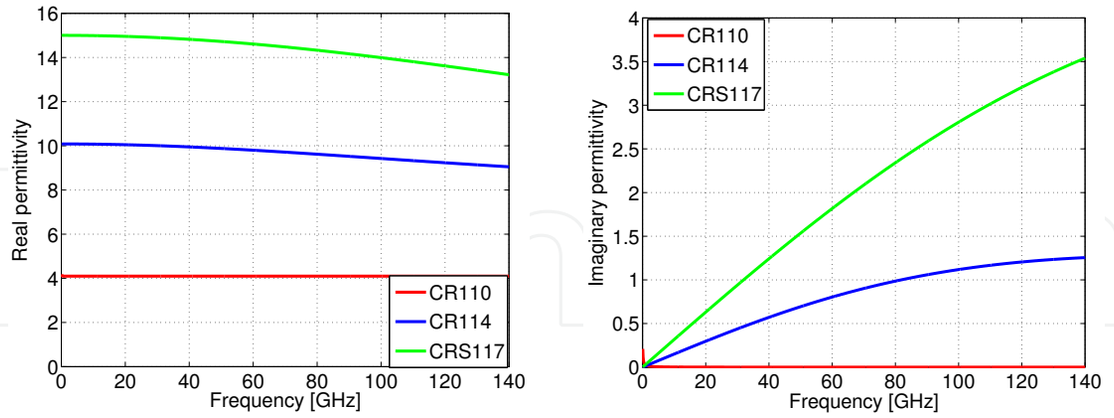

(a) (b)

Figure 9. Real and imaginary parts of retrived permittivity of Eccosorb samples.

5.4. Extracted permittivity of epoxies Stycast W19 and Stycast 2850 FT

Commercially available epoxies Stycast W19 ans Stycast 2850FT can be used as matrices in the synthesis of microwave absorbing materials. Carbonyl iron or steel particles can be used as

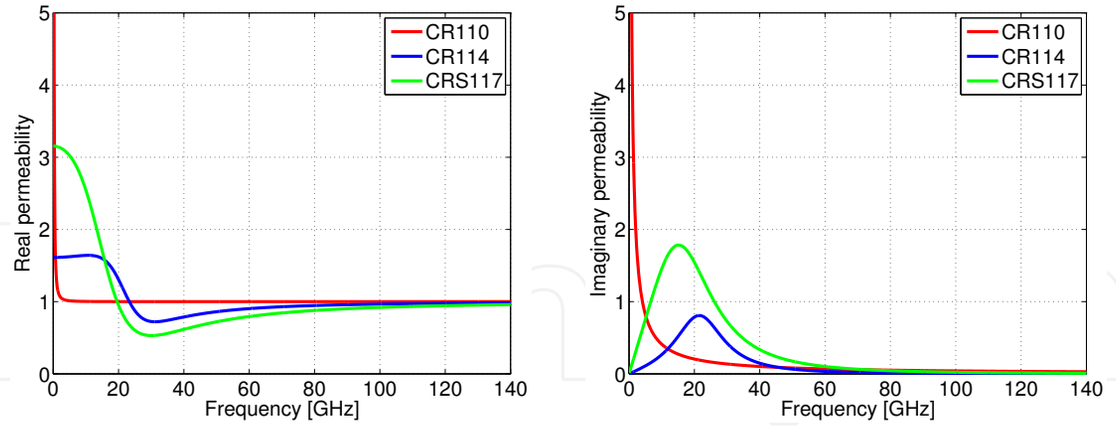

(a) (b)

Figure 10. Real and imaginary parts of retrived permeability of Eccosorb samples.

fillers. The differences between two epoxies are in viscosity, dielectric and thermal properties. Stycast 2850FT epoxy is loaded with alumina for the higher thermal conductivity. Alumina loading makes Stycast 2850FT epoxy more viscose than Stycast W19, thus implying lower filling fraction of possible absorbing particles. Stycast W19 exhibits lower viscosity and lower thermal conductivity than Stycast 2850FT. In terms of dielectric properties, Stycast 2850FT exhibits higher real permittivity and losses than Stycast W19.

Mentioned epoxies are dielectrics and have one relaxation frequency at microwave frequencies. In order to extract frequency dependent permittivity, we model it with simple Debye model (Eq. (10)). With the same procedure described in section 5.2, we extract high frequency permittivity model of both Stycast W19 and Stycast 2850FT.

Figure 11 (a) represents measured and fitted S_{21} of Stycast 2850FT in W band. Figure 11 (b) represents measured S_{21} of Stycast 2850FT in Ka band together with simulations performed with extracted permittivity model from W band. Good agreement is achieved. Figure 12

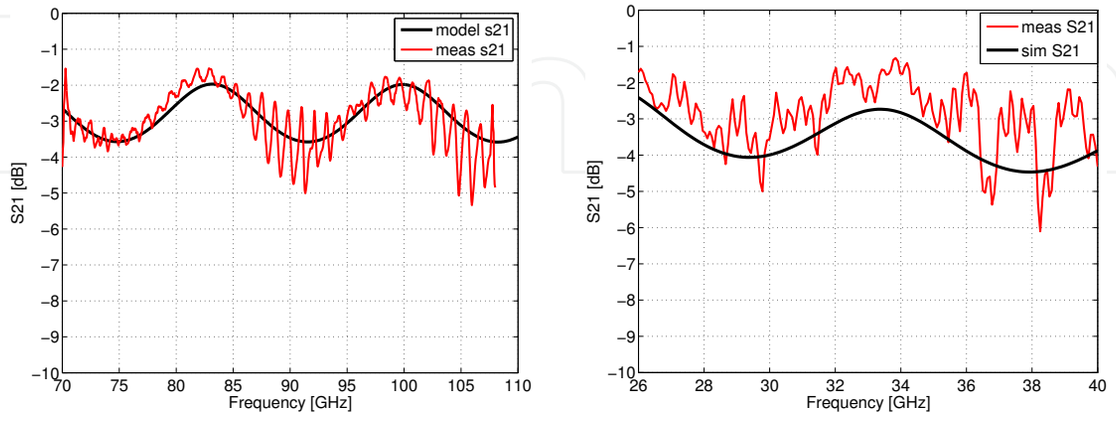

(a) (b)

Figure 11. Measured and fitted S_{21} of Stycast 2850FT epoxy in W band (a) and measured and simulated S_{21} in Ka band (b).

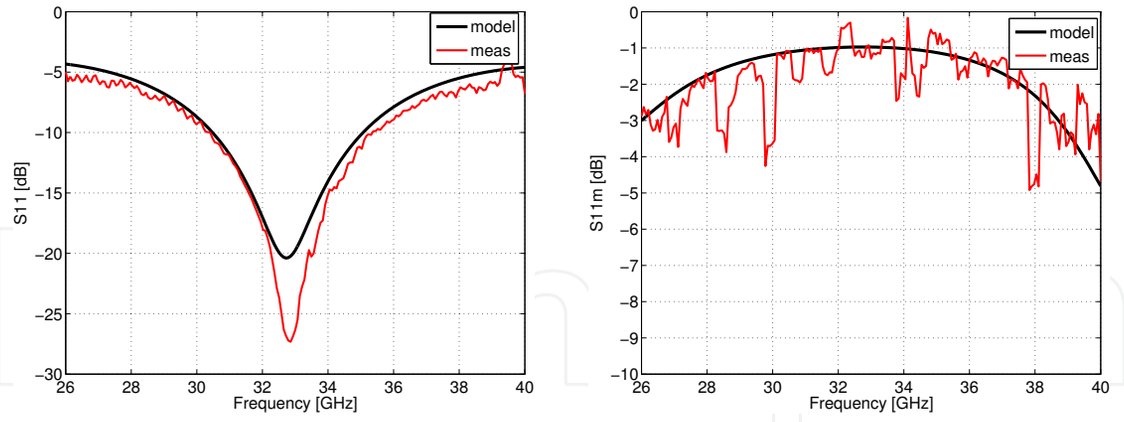

Figure 12. Measured and simulated reflection coefficient of Stycast 2850FT epoxy samples without (a) and with (b) metal backing. Good agreement between measurements and simulations is obtained which validate extracted permittivity model.

represents measured and simulated reflection of Stycast 2850FT with and without metal backing in Ka band. There is a good agreement between measured and simulated data which is proof for correctness of the extracted model. Figure 13 represents extracted real and imaginary frequency dependent permittivity of examined epoxies. Conclusion is that in the case of dielectric materials whose permittivity model exhibits one relaxation frequency in microwave frequencies, permittivity model extracted from the fitting at high frequencies is also valid at low frequencies.

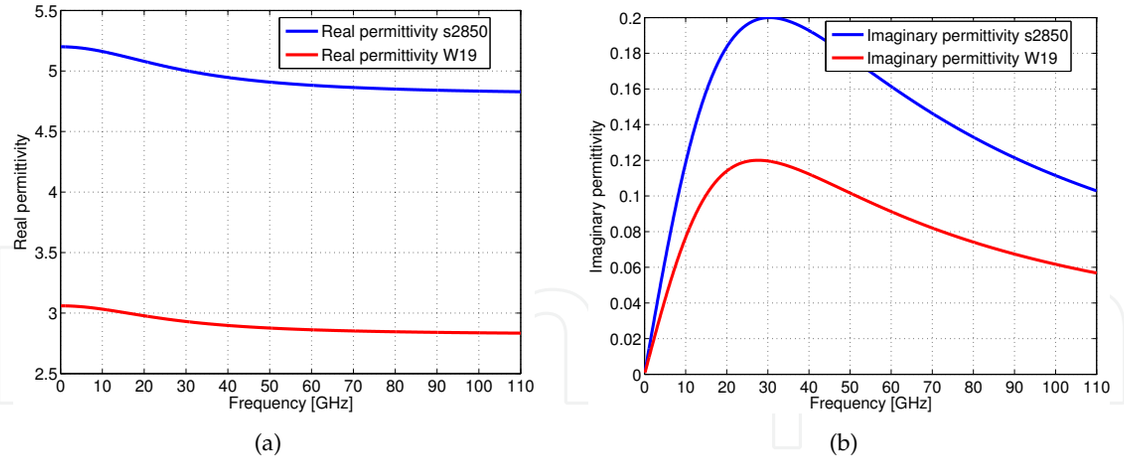

Figure 13. Real and imaginary permittivity extracted from the fitting for both Stycast W19 and Stycast 2850FT.

6. Conclusions

In this Chapter, we described a method for the extraction of frequency dependent permittivity and permeability parameters of magnetically loaded absorbing materials from free space transmission measurements. Our approach can be applied to noisy data and do not need any

parameter to be known in advance. The starting assumption is based on the consideration of a two composite material (dielectric matrix and magnetic particles). According to ([8]) about models that represent composite materials, dielectric property of our samples was modeled with simple Debye relaxation model, while complex permeability was modeled with Lorenzian resonant model. Important thing was that we restored first permittivity models of the samples by fitting at high frequencies where permeability is constant and equal 1. After that step we did fitting at low frequencies to extract permeability model. The proposed method is also suitable for permittivity extraction of dielectric materials in those situations where no *a priori* information is known about material, except that material is two composite, homogeneous and isotropic. Also, for the first time we presented extracted complex and frequency dependent values of permittivities and permeabilities of Eccosorb absorbing materials (CR110, CR114 and CRS117) in the frequency range from 22 to 140 GHz. Since below 22 GHz we did not perform scattering parameters measurements and fitting, we can not say if the extracted models are also valid in that region. Future work will include investigation of permittivity and permeability frequency dependence at low frequencies (from 0 up to 22 GHz) and from 150 to 650 GHz.

Author details

Irena Zivkovic and Axel Murk
Institute of Applied Physics, University of Bern, Switzerland

7. References

[1] Bunget, I. (1984). *Physics of solid dielectrics*, Materials science monographs 19, Elsevier.
[2] Choi, H. D. et al. (1998). Frequency Dispersion Characteristics of the Complex Permittivity of the Epoxy Carbon Black Composites, *Journal of Applied Polymer Science* Vol.67.
[3] Jarvis, J. B. (1990). Transmission Reflection and Short Circuit Line Permittivity Measurements, *NIST* Technical Note 1341.
[4] Jarvis, J. B. et al. (1992). A non-linear least squares solution with causality constraints applied to transmission line permittivity and permeability determination, *IEEE Transactions on Instrumentation and Measurements* Vol. 41.
[5] Jarvis, J. B. et al. (2005). Measuring the permittivity and permeability of lossy materials: Solids, Liquids, Building Material and Negative-Index Materials, *NIST* Technical Note 1536.
[6] Kittel, C. (1946). Theory of the dispersion of magnetic permeability in ferromagnetic materials at microwave frequencies, *Physical Review* Vol.70.
[7] Rado, G. T., Wright, R. W.& Emerson, W. H. (1950). Ferromagnetism at very high frequencies. Two mechanisms of dispersion in a ferrite, *Physical Review* Vol. 80.
[8] Sihvola, A. (1999). *Electromagnetic Mixing Formulas and Applications*, The Institution of Electrical Engineers, London, UK.
[9] Zhuravlev, V. A. &Suslyaev V. I. (2006a). Physics of magnetic phenomena analysis and correction of the magnetic permeability spectra of Ba3Co2Fe24O41 hexaferrite by using Kramers-Kronig relations, *Russian Physics Journal* Vol. 49: No. 8.

[10] Zhuravlev, V. A. &Suslyaev V. I. (2006b). Analysis of the microwave magnetic permeability spectra of ferrites with hexagonal structure, *Russian Physics Journal* Vol. 49: No. 9.

IntechOpen